Super slowing down in the bond-diluted Ising model

Wei Zhong,* Gerard T. Barkema, and Debabrata Panja
Department of Information and Computing Sciences, Utrecht University, Princetonplein 5, 3584 CC Utrecht, The Netherlands

(Received 17 February 2020; accepted 3 August 2020; published 24 August 2020)

In models in statistical physics, the dynamics often slows down tremendously near the critical point. Usually, the correlation time τ at the critical point increases with system size L in power-law fashion: $\tau \sim L^z$, which defines the critical dynamical exponent z. We show that this also holds for the two-dimensional bond-diluted Ising model in the regime $p > p_c$, where p is the parameter denoting the bond concentration, but with a dynamical critical exponent $z(p)$ which shows a strong p dependence. Moreover, we show numerically that $z(p)$, as obtained from the autocorrelation of the total magnetization, diverges when the percolation threshold $p_c = 1/2$ is approached: $z(p) - z(1) \sim (p - p_c)^{-2}$. We refer to this observed extremely fast increase of the correlation time with size as *super slowing down*. Independent measurement data from the mean-square deviation of the total magnetization, which exhibits anomalous diffusion at the critical point, support this result.

DOI: 10.1103/PhysRevE.102.022132

I. INTRODUCTION

The Ising model has proven to be a staple model in physics for studying phase transitions and critical phenomena [1,2]. The model was originally conceived to provide a theoretical understanding of the existence of a Curie temperature for "pure" ferromagnetic materials; purity here refers to the fact that all throughout the material, every lattice site contains a spin, and every spin interacts uniformly with the surrounding ones. From that point of view, it can be argued that, in nature, pure materials are rare, i.e., impurities are by and large inevitable.

In the Ising model, the impurities have been implemented in terms of randomly placed nonmagnetic spins (site-diluted Ising model) [3–7] or missing interactions (bond-diluted Ising model) [8–12]. The inclusion of any kind of randomness into the system can have significant effects on its critical properties [13]. For instance, a new universality class was found in the three-dimensional bond-diluted Ising model [14,15], and complex logarithmic corrections for the equilibrium properties were observed [7,16]. Moreover, a large number of novel crossover behaviors between pure and percolating Ising systems have been found [17–22]. Also, the dynamics at the percolation threshold is discussed in Refs. [23,24] and the dynamical exponent for spin systems with random dilution or randomness in the coupling constants has been considered in Refs. [25–29]. Despite these advances, dynamical properties of the bond-diluted Ising model (i.e., as a function of bond concentration p) remains poorly studied.

In this paper, we study the slowing down of the dynamics of the total magnetization autocorrelation function at the critical temperature $T_c(p)$ in the square $(L \times L)$ two-dimensional bond-diluted Ising model with Monte Carlo simulations. To this end, by using the Binder cumulant, we first measure $T_c(p)$ at several values of p. We then turn to the calculation of $z(p)$ for several $p > p_c$ from the total magnetization autocorrelation function: by collapsing this autocorrelation function to a reference curve, we calculate the relative terminal exponential decay time $\tau[T_c(p)]$ for the correlation function. Thereafter, by fitting this data as $\tau[T_c(p)] \sim L^{z(p)}$, we directly extract $z(p)$. As $p \to p_c^+$, we empirically find that the dynamical exponent $z(p)$ increases continuously as $z(p) - z(1) \sim (p - p_c)^{-2}$, with $z(1) = 2.1665(12)$ the dynamical critical exponent of the ordinary Ising model [30].

Furthermore, we also consider the mean-square deviation (MSD) of the total magnetization M of the model, which for $p = 1$ has been shown to exhibit anomalous diffusion as $\langle \Delta M^2(t) \rangle \sim t^\alpha$ with the anomalous exponent $\alpha = \frac{\gamma}{\nu z(1)}$ [31], with $\gamma = 7/4$ and $\nu = 1$. Given that the equilibrium critical exponents γ and ν are numerically nearly independent of p for $p \geqslant 0.6$ [32], combined with values for $z(p)$ as obtained through the terminal relaxation time for different p, the various MSD curves of the total magnetization are collapsed on top of each other with a p-dependent shift factor $\mathcal{G}(p)$ via $\ln(\langle \Delta M^2 \rangle / L^{2+\gamma/\nu})/\alpha(p) \sim \ln(t/L^{z(p)}) + \ln[\mathcal{G}(p)]/\alpha(p)$, with $\alpha(p) = \gamma(p)/[\nu(p)\, z(p)]$. The result reveals that the magnetization indeed experiences anomalous diffusion at the critical point, for a range of dilution $p > p_c$. The collapse of the MSD of the magnetization confirms that the measured values of $z(p)$ are correct.

The paper is organized as follows: In Sec. II we introduce the two-dimensional (2D) bond-diluted Ising model and measure its critical temperature at several values of p. In Sec. III we obtain the dynamical exponent $z(p)$ from the total magnetization autocorrelation function. In Sec. IV, we confirm $z(p)$ values from the exponent of anomalous diffusion of the MSD of the total magnetization. We conclude the paper in Sec. V.

*w.zhong1@uu.nl

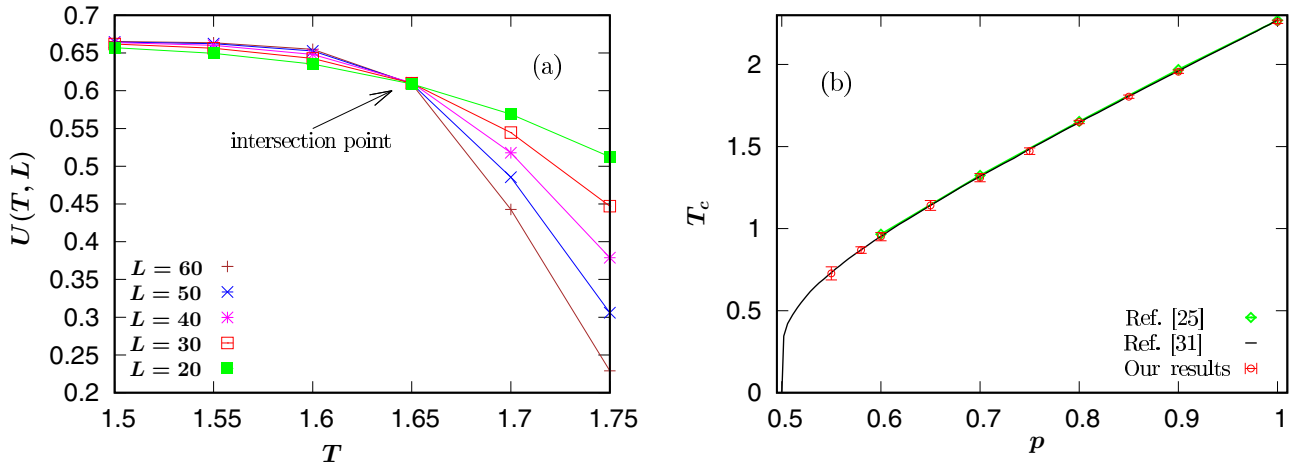

FIG. 1. (a) Example calculation of $T_c(p)$ for the 2D bond-diluted Ising model for $p = 0.8$ using Binder cumulant. The x value of the intersection point indicates that $T_c(p = 0.8) = 1.650 \pm 0.020$. (b) Critical temperatures for different values of p, as noted in Table I. Our results match those of Refs. [32,38] very well.

II. BOND-DILUTED ISING MODEL AND ITS CRITICAL TEMPERATURE

We consider the two-dimensional (2D) bond-diluted Ising model on an $L \times L$ square lattice with periodic boundary conditions. For this model, the Hamiltonian, without an external field, is given by

$$\mathcal{H} = -\sum_{\langle ij \rangle} J_{ij} s_i s_j, \tag{1}$$

where $s_i = \pm 1$ is the spin residing at site i, $\langle ij \rangle$ denotes the sum running over all nearest-neighbor sites, and the coupling constant J_{ij} is given by the distribution function

$$P(J_{ij}) = p\delta(J_{ij} - 1) + w(1 - p)\delta(J_{ij}), \tag{2}$$

with p being the bond concentration ($0 \leqslant p \leqslant 1$). The function (2) simply means that the value of J_{ij} is 1 with probability p, and 0 otherwise.

For the pure Ising model ($p = 1$), there is a second-order phase transition at $T_c(1) = 2/\ln(1 + \sqrt{2})$ [33]. When p reaches the percolation threshold $p_c = 1/2$, its critical temperature decreases to zero: $T_c(p_c) = 0$ [34]. To determine $T_c(p)$ for in-between values of p, we use the Binder cumulant. It is defined as [35]

$$U(T, L) = 1 - \frac{\langle M^4 \rangle}{3\langle M^2 \rangle^2}, \tag{3}$$

where $\langle M^4 \rangle$ and $\langle M^2 \rangle$ are the thermal averages of the fourth and second moments of the total magnetization $M = \sum_{i=1}^{L \times L} s_i$. For each value of p, the curves of $U(T, L)$ plotted vs T for various values of L intersect at a fixed point, which determines the critical temperature. The process is illustrated in Fig. 1(a).

We perform Monte Carlo simulations by using the Wolff algorithm [36,37] to calculate $T_c(p)$. Running many independent samples provide us with fairly accurate values of these critical temperatures, as noted in Table I. In Fig. 1(b) we show that the values for $T_c(p)$ obtained this way match very well with those in Refs. [32,38].

III. DYNAMICAL EXPONENT FOR DIFFERENT VALUES OF p

Having obtained the critical temperatures for a number of p values as per above, in this section, we measure the total magnetization autocorrelation function $\langle M(t) \cdot M(0) \rangle$. To do so, we first run 2×10^6 Wolff Moves to thermalize the system. Subsequently, we evolve the system following Glauber dynamics, i.e., spin flips are proposed at random locations and accepted with the Metropolis acceptance probability. Time is measured in terms of attempted Monte Carlo moves, since every spin attempts to flip statistically once per unit time. As we continue to do so, we keep taking snapshots of the full system at regular intervals over a total time of 2×10^7 attempted Monte Carlo moves per lattice site, and correspondingly compute the total magnetization M at every snapshot. This leads us to $\langle M(t) \cdot M(0) \rangle$. For different values of p, we run 500 to 2000 independent simulations to achieve decent accuracy. We vary the system size from 10 to 40.

For a given value of p and the corresponding critical temperature $T_c(p)$, we collapse all the curves for the normalized total magnetization autocorrelation

TABLE I. Number of samples $N(p)$ used to measure $T_c(p)$, and the simulation results for $T_c(p)$ (including error bars) for different bond concentrations p.

p	0.9	0.85	0.8	0.75	0.7	0.65	0.6	0.58	0.55
N	2000	5000	20 000	20 000	20 000	20 000	200 000	200 000	400 000
T_c	1.956(10)	1.804(10)	1.650(20)	1.472(20)	1.310(25)	1.141(30)	0.951(20)	0.869(25)	0.727(40)

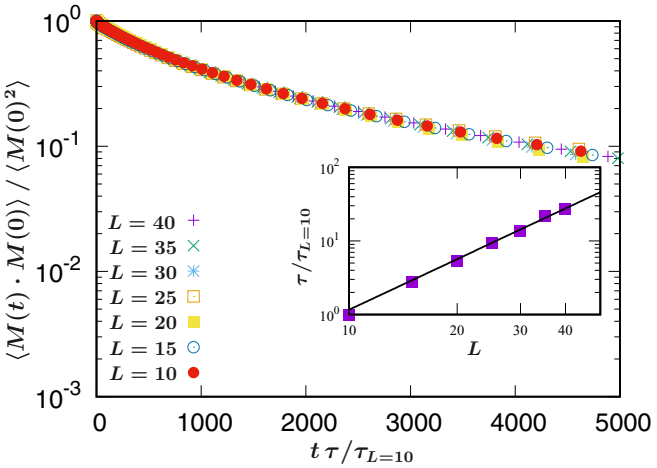

FIG. 2. The collapse of $\langle M(t)\cdot M(0)\rangle/\langle M(0)^2\rangle$ as a function of $t\tau[T_c(p)]/\tau[T_c(p)]_{L=10}$ for $p = 0.8$. The system size varies from 10 to 40. Inset: correspondingly, $\tau[T_c(p)]/\tau[T_c(p)]_{L=10}$ as a function of L. The dynamical exponent is obtained by fitting these data as $\tau[T_c(p)]/\tau[T_c(p)]_{L=10} \sim L^{z(p)}$. The solid line corresponds the function $y = x^{2.285}$. From this we obtain $z(0.8) \approx 2.285$.

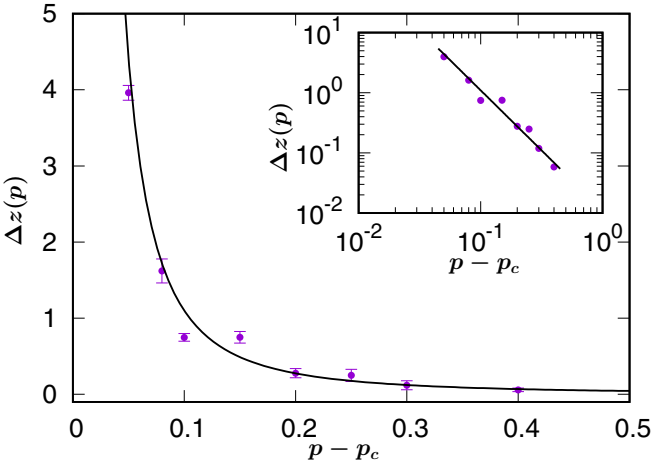

FIG. 3. The dynamical exponent difference $\Delta z(p) = z(p) - z(1)$ as a function of $p - p_c$, where $z(1) = 2.1665(12)$ [30] is the dynamical exponent for the pure 2D Ising model. The result implies that $z(p) \to \infty$ as $p \to p_c^+$.

function $\langle M(t)\cdot M(0)\rangle/\langle M(0)^2\rangle$ to a reference curve ($L = 10$). This allows us to compute the ratio of the terminal decay times $\tau[T_c(p)]/\tau[T_c(p)]_{L=10}$. Figure 2 demonstrates this procedure for $p = 0.8$: with a properly chosen value of $\tau[T_c(p)]/\tau_{L=10}[T_c(p)]$, the $\langle M(t)\cdot M(0)\rangle/\langle M(0)^2\rangle$ data for different system sizes collapse on the curve corresponding to $L = 10$.

Furthermore, given our argument in Appendix A that L is the characteristic length scale for $L \geqslant 10$ for the 2D bond-diluted Ising model when $p \geqslant 0.6$, we have, at the critical temperature,

$$\tau(p)/\tau_{L=10}(p) \sim L^{z(p)}. \tag{4}$$

By plotting the $\tau(p)/\tau_{L=10}(p)$ data (inset Fig. 2), we extract $z(p)$. The results from this exercise for several values of p are shown in Fig. 3. Numerically, therein we find that

$$\Delta z(p) = z(p) - z(1) \sim (p - p_c)^{-2} \text{ for } p_c < p < 1, \tag{5}$$

where $z(1) = 2.1665(12)$ [30] is the dynamical exponent for the pure 2D Ising model.

Based on concepts of renormalization, we anticipated that, away from the percolation threshold p_c, the correlation time as a function of system size would show a crossover from the behavior for the bond-diluted Ising model at small system sizes to that of the ordinary Ising model at large system sizes, with a crossover size that diverges if p_c is approached. Instead, we find a fairly clean power-law behavior of the correlation time for all system sizes, with a single exponent $z(p)$ that varies strongly with p. As a function of bond dilution p, the dynamical exponent $z(p)$ increases monotonically when p decreases from $p = 1$ to $p = p_c$. Moreover, the numerical results suggest that $z(p)$ will become infinitely large when p approaches the percolation threshold $p \to p_c^+$, i.e., the dynamics of the system gets extremely slow as $p \to p_c^+$, a phenomenon we term "super slowing down."

IV. ANOMALOUS DIFFUSION OF THE TOTAL MAGNETIZATION

To confirm the observed behavior of super slowing down [i.e., Eq. (5)] for the bond-diluted Ising model by means of independent measurements, we now focus on the mean-square deviation (MSD) of the magnetization as a function of time t as

$$\langle \Delta M^2 \rangle = \langle [M(t) - M(0)]^2 \rangle. \tag{6}$$

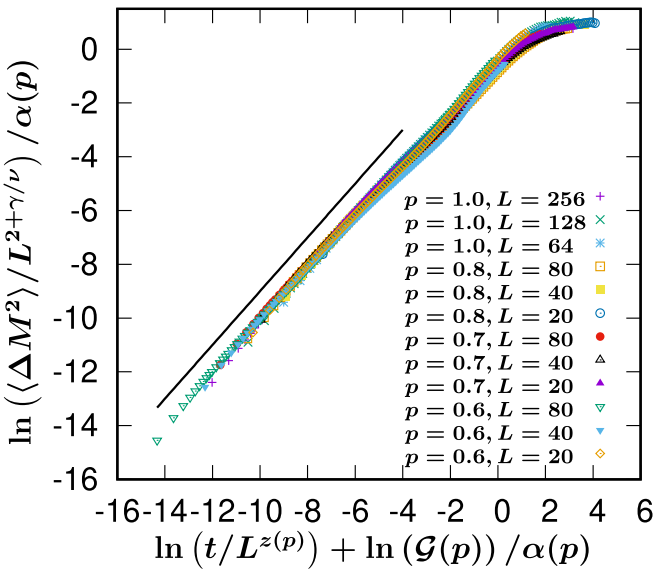

FIG. 4. The collapse of the mean-square displacement of the total magnetization via $\ln(\langle \Delta M^2\rangle/L^{2+\gamma/\nu})/\alpha(p) \sim \ln(t/L^{z(p)}) + \ln[\mathcal{G}(p)]/\alpha(p)$, where the obtained values of $z(p)$ from the last section are employed and $\mathcal{G}(p)$ is a p-dependent shift factor. The slope of the solid line is unity. It confirms that the MSD of the total magnetization experiences anomalous diffusion at $T_c(p)$ and the values of $z(p)$ is increasing when $p \to p_c+$.

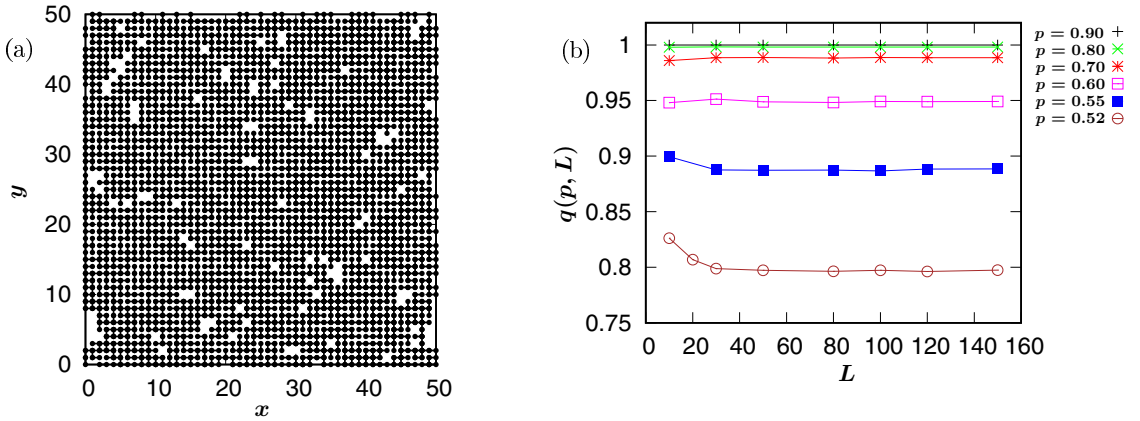

FIG. 5. (a) A snapshot of the biggest knot cluster for $L = 50$ and $p = 0.6$. Spins that are not belong to this cluster are represented by cavities. (b) Plot of $q(p, L) = \langle S(p, L)\rangle/L^2$ for various values of p and L: for $p \geqslant 0.6$, $q(p, L)$ is independent of L for $L \geqslant 10$.

At short times ($t \approx 1$), changes in M, occurring due to random thermal fluctuations of individual spins, are uncorrelated; hence $\langle \Delta M^2\rangle \sim L^2 t$ for the 2D Ising model. At long times, $t \gtrsim L^{z(p)}$, we expect $\langle M(t) \cdot M(0)\rangle = 0$, meaning that

$$\langle \Delta M^2\rangle \underset{t\gtrsim L^{z(p)}}{=} 2\langle M(t)^2\rangle \sim L^{2+\gamma(p)/\nu(p)}. \tag{7}$$

If we assume that the MSD is given by a simple power law in the intermediate-time regime ($1 \lesssim t \lesssim L^{z(p)}$), then we obtain

$$\langle \Delta M^2\rangle \sim L^{2+\gamma(p)/\nu(p)} (t/L^{z(p)})^{\alpha(p)}, \tag{8}$$

where $\alpha(p) = \frac{\gamma(p)}{\nu(p)z(p)}$. For the pure Ising model in two dimensions ($p = 1$), we have shown that [31]

$$\langle \Delta M^2\rangle/L^{2+\gamma/\nu} = f(t/L^z), \tag{9}$$

where $\gamma = 7/4$ and $\nu = 1$ are two equilibrium critical exponents. Here $f(x)$ is a scaling function such that $\lim_{x\to 0} f(x) \sim x^{\gamma/(\nu z)} \approx x^{0.81}$, and $f(x)$ saturates for $x \gtrsim 1$. Indeed, given that $\gamma(p)$ and $\nu(p)$ are nearly independent of p when $p \geqslant 0.6$

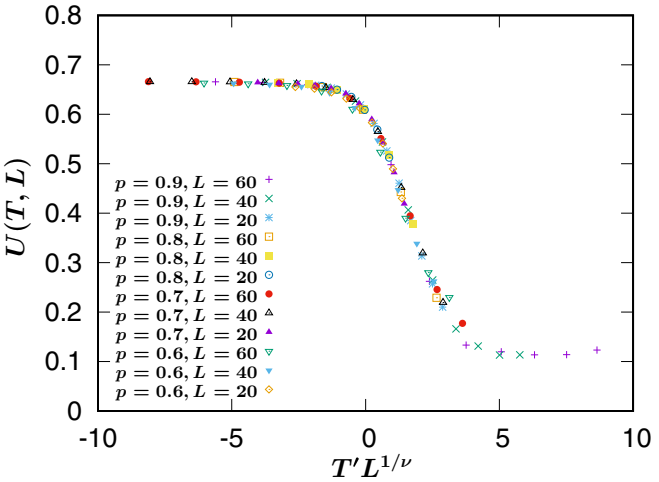

FIG. 6. The Binder cumulant for $p \geqslant 0.6$. The data are collapsed as $U(T, L) \sim f(T'L^{1/\nu(p)})$ for different p and L, where $T' = (T - T_C)/T_C$ is the reduced temperature. Here $L = 20$, 40, and 60 for each bond concentration, and we set all $\nu(p) = 1.0$ to collapse the data.

[32] (see also Appendix B), if the scaling relation (9) also continues to hold for values of p other than unity, then we can use it to obtain independent confirmation for the super slowing down (5). We demonstrate this below by focusing on $p \geqslant 0.6$.

Since in the previous section we obtained the values of $z(p)$ for different p, here, we describe the MSD of the total magnetization by modifying Eq. (8) as

$$\langle \Delta M^2\rangle/L^{2+\gamma/\nu} \sim \mathcal{G}(p)(t/L^{z(p)})^{\alpha(p)}, \tag{10}$$

where $\mathcal{G}(p)$ is a p-dependent shift factor. We take *logarithm* of both sides of Eq. (10) to write

$$\ln(\langle \Delta M^2\rangle/L^{2+\gamma/\nu})/\alpha(p) \sim \ln(t/L^{z(p)}) + \ln[\mathcal{G}(p)]/\alpha(p). \tag{11}$$

Suppose we choose the MSD of the total magnetization for the normal Ising model as the reference [this means that $\mathcal{G}(1) \equiv 1$] if the values of $z(p)$ obtained from the last section are correct; then with these $z(p)$ values and the shift factor $\mathcal{G}(p)$, the MSD of the total magnetization for different p can be made to collapse onto the data for $p = 1$ via Eq. (11).

To obtain the $\langle \Delta M^2(t)\rangle$ data, once again, we first thermalize the system with 2×10^6 Wolff moves, then measure $\langle \Delta M^2\rangle$ in a further simulation over 2×10^7 attempted Monte Carlo moves per lattice site. We use three different system sizes: $L = 20$, 40, 60 for every value of p.

Figure 4 implies that by using the values of $z(p)$ obtained from the last section, indeed for different p, the MSD of the magnetization can be collapsed onto the data for $p = 1$ via Eq. (11). It confirms that the MSD of the total magnetization experience anomalous diffusion at $T_c(p)$ and $z(p)$ values obtained from the terminal relaxation time are correct.

In summary, with two different methods, we have shown that $z(p)$ is diverging when $p \to p_c^+$, i.e., the dynamics of the system is getting extremely slow when we reduce the bond concentration to its percolation threshold. We do not have a quantitative explanation for this behavior. That said, it might arise from the fact that the fraction of "unhappy" bonds (active bonds between sites with opposing spin values) at the critical temperature decreases to zero if p_c is

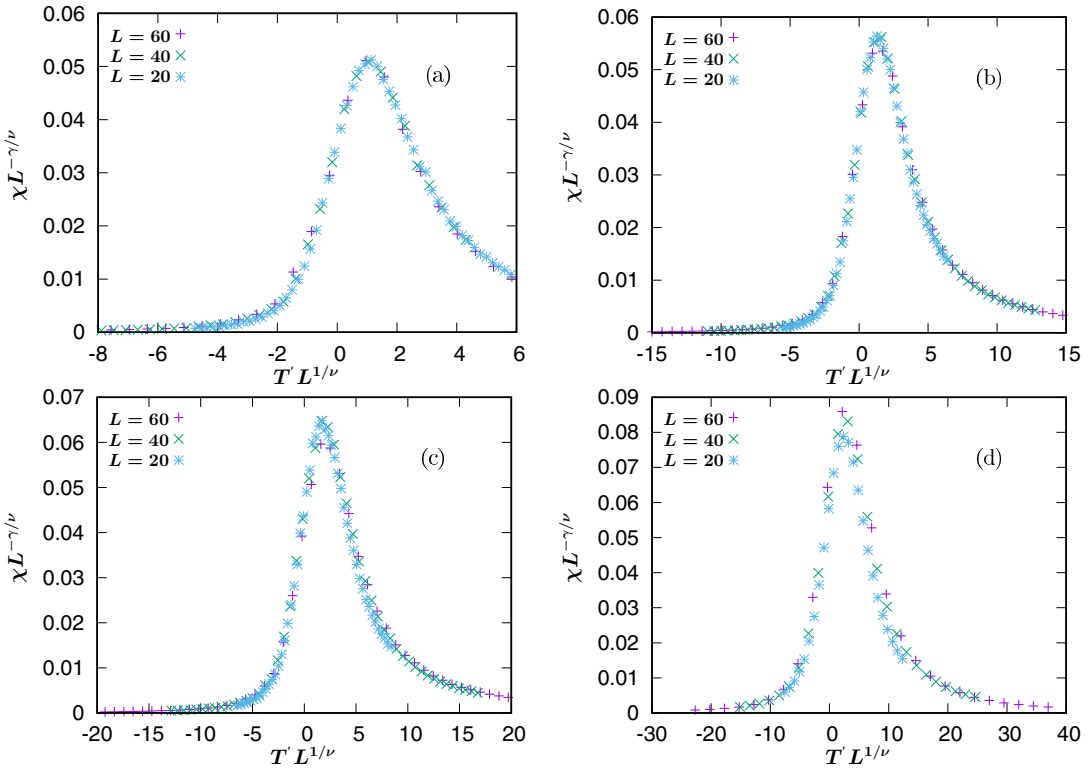

FIG. 7. The scaling of magnetic susceptibility as a function of reduced temperature: $\chi L^{-\gamma/\nu} = \tilde{\chi}(T'L^{1/\nu})$. Here $\tilde{\chi}$ is a dimensionless function, the values of $\gamma(p)$ and $\nu(p)$ are chosen to be their values for the normal Ising model, i.e., $\gamma(p) = 1.75$ and $\nu(p) = 1$. For panels (a)–(d), the bond concentrations are $p = 0.9$, 0.8, 0.7, and 0.6, respectively. The good collapse of all the data indicates that both γ and ν are numerically indistinguishable for $p \geqslant 0.6$.

approached, thereby removing the energetic contribution of restoring forces; we provide some measurements for this in Appendix C.

V. DISCUSSION

In this paper, we study the critical dynamical exponent $z(p)$ for the 2D bond-diluted Ising model with bond concentration p. We first measure the critical temperature $T_c(p)$ for different bond concentrations p by using the Binder cumulant. We then calculate the relative values of the terminal decay time τ by collapsing the total magnetization autocorrelation function to a reference value, from which we obtain $z(p)$ using the relation $\tau \sim L^{z(p)}$.

We find that $z(p)$ increases when $p \to p_c^+$ as the power law $z(p) - z(1) \sim (p - p_c)^{-2}$, which we refer to as super slowing down. We confirm this result from independent measurements of the MSD of the total magnetization that exhibits anomalous diffusion.

Our results indicate that $z(p) \to \infty$ as $p \to p_c^+$. This leaves us with the interesting question: what happens to $z(p)$ when $p < p_c$? We plan to explore this in the future.

ACKNOWLEDGMENT

W.Z. acknowledges financial support from the China Scholarship Council (CSC).

APPENDIX A: RELEVANT LENGTH SCALE FOR CRITICAL PHENOMENA OF THE BOND-DILUTED ISING MODEL

In the pure 2D Ising model of dimension $L \times L$, the only relevant length scale for critical phenomena is L. For the bond-diluted Ising model there are other length scales, for instance, corresponding to the size of the biggest cluster, $S(p, L)$. Here, a cluster is defined is by the set of spins such that there is at least one continuous (bond-following) path from every spin in the cluster to every other spin in the same cluster. We define the size of the cluster by the total number of spins belonging to the cluster [thus $S(p, L)$ is the number of spins in the biggest cluster for an $L \times L$ system with bond concentration p].

In Fig. 5(b) the quantity considered is $q(p, L) = \langle S(p, L)\rangle/L^2$. If this quantity is independent of L then it means that there is no difference between the two differently defined length scales (apart from a scaling factor). For each result, we have generated 500 samples. We see in Fig. 5(b) that, for $p \geqslant 0.6$, $q(p, L)$ is independent of L for $L \geqslant 10$. This means that for the range of dilution $p \geqslant 0.6$ used in this paper, we can use L as the relevant length scale for critical phenomena provided $L \geqslant 10$.

APPENDIX B: EQUILIBRIUM CRITICAL EXPONENTS ν AND γ

In this Appendix, we show that the equilibrium critical exponents ν and γ for the bond-diluted Ising system with

$p \geqslant 0.6$ are numerically indistinguishable from their values in the pure Ising model.

We note here that, according to the Harris criterion [39], if the correlation length critical exponent ν fulfills the inequality $\nu \geqslant 2/d$ where d is the spatial dimensionality, then disorder does not affect the critical behavior. For the 2D Ising model, $\nu = 1$ is marginal, which translates into logarithmic corrections to some critical exponents. In the pure Ising model, the exponents γ and ν do not show logarithmic corrections, and our numerical results shown in this Appendix indicate that the ratio of γ and ν is unchanged in the regime we studied, for $p \geqslant 0.6$, without logarithmic corrections. Also, the Binder cumulant does not show logarithmic corrections. This is not obvious, and in fact there are reports of logarithmic corrections to the equilibrium properties of the diluted spin systems [5,7,40]. We cannot rule out the possibility of having logarithmic corrections in the quantities measured by us, as these are difficult to observe in simulations.

First, if we get the values of T_c for different p, the Binder cumulant can be scaled as

$$U(T, L) \sim f(T' L^{1/\nu(p)}), \tag{B1}$$

which will provide us the value of $\nu(p)$. Here $T' = (T - T_C)/T_C$ is the reduced temperature.

In Fig. 6, we collapse the data of $U(L, T)$ for $L = 20$, 40, and 60 with $\nu(p) \approx 1$. It indicates that $\nu(p)$ is numerically indistinguishable from unity for $p \geqslant 0.6$.

Next, we turn to measure the magnetic susceptibility χ. For this simulation, we have used 500 independent samples for each value of p. It is a well-known result [37] that the susceptibility can be scaled as

$$\chi L^{-\gamma/\nu} = \tilde{\chi}(T' L^{1/\nu}), \tag{B2}$$

where $\tilde{\chi}$ is a dimensionless function.

After rescaling the susceptibility using Eq. (B2), the data shown in Fig. 7 demonstrate that γ is numerically indistinguishable from $7/4$ for $p \geqslant 0.6$.

In other words, in this Appendix we have shown that γ and ν are numerically indistinguishable respectively from $7/4$ and unity for $p \geqslant 0.6$, confirming the results from Ref. [32].

APPENDIX C: NUMBER OF DIFFERENT TYPES OF BONDS

In this Appendix, we connect the super slowing down in the 2D bond-diluted Ising model with its equilibrium property, i.e., the ensemble average of the number of unhappy bonds, i.e., the number of interacting nearest-neighbor spins with opposite signs at the critical temperature.

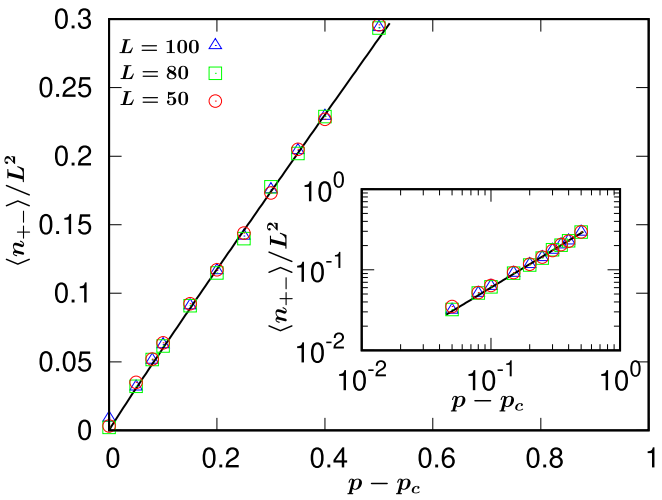

FIG. 8. The value of $\langle n_{+-}\rangle$ as a function of $p - p_c$ for $L = 50$, 80, and 100. The solid line goes as $\sim(p - p_c)^{0.97}$. The inset is a log-log plot of the data. It suggests that when $p \to p_c^+$, $\langle n_{+-}\rangle \to 0$, then most of the bonds are activated so that nearly all spins are unlikely to flip, resulting in the super slow dynamics of the system.

In the bond-diluted Ising model, we distinguish inactive bonds (with $J_{ij} = 0$), active bonds connecting sites with aligned spins, and active bonds that connect sites with spins of opposite signs. For the active bonds, we denote the numbers of those aligned and nonaligned spins by $(n_{++} + n_{--})$ and n_{+-}, respectively. Energetically, $\langle n_{++}\rangle$ and $\langle n_{--}\rangle$ are the bonds that try to keep the system as it is, and $\langle n_{+-}\rangle$ is driving spins to flip. If $\langle n_{+-}\rangle$ decreases, then most of the proposed spin flips will be rejected and the dynamics of the system will get slower.

In our simulations, we have performed 100 independent samples to obtain the number of unhappy bonds. The measured values of $\langle n_{+-}\rangle$ at the critical temperature can be found in Fig. 8, with a log-log plot as an inset. In particular, we find numerically that

$$\langle n_{+-}\rangle/L^2 \sim (p - p_c)^{0.97\pm0.03} \text{ for } p \geqslant p_c. \tag{C1}$$

When $p \to p_c^+$, the values of $\langle n_{+-}\rangle$ reduces to zero (or a value close to zero), which means that most of the active bonds are "happy" so that spins are unlikely to flip. This might explain why the system is getting super slow when p approaches the percolation threshold.

[1] H. E. Stanley, *Phase Transitions and Critical Phenomena* (Clarendon Press, Oxford, 1971).
[2] P. C. Hohenberg and B. I. Halperin, Rev. Mod. Phys. **49**, 435 (1977).
[3] H. G. Ballesteros *et al.*, J. Phys. A: Math. Gen. **30**, 8379 (1997).
[4] H. G. Ballesteros, L. A. Fernandez, V. Martin-Mayor, A. Munõz Sudupe, G. Parisi, J. J. Ruiz-Lorenzo, Phys. Rev. B **58**, 2740 (1998).
[5] P. H. L. Martins and J. A. Plascak, Phys. Rev. E **76**, 012102 (2007).
[6] J.-K. Kim and A. Patrascioiu, Phys. Rev. Lett. **72**, 2785 (1994).
[7] R. Kenna and J. J. Ruiz-Lorenzo, Phys. Rev. E **78**, 031134 (2008).
[8] B. N. Shalaev, Phys. Rep. **237**, 129 (1994).
[9] C. Jayaprakash, E. K. Riedel, and M. Wortis, Phys. Rev. B **18**, 2244 (1978).

[10] Y. L. Loh and E. W. Carlson, Phys. Rev. Lett. **97**, 227205 (2006).
[11] M. Hasenbusch, F. Parisen Toldin, A. Pelissetto, and E. Vicari, Phys. Rev. E **78**, 011110 (2008).
[12] A. R. Rivera, G. A. Perez Alcazar, and J. A. Plascak, Phys. Rev. B **41**, 4774 (1990).
[13] E. Albayrak, Commun. Theor. Phys. **68**, 361 (2017).
[14] M. Hasenbusch, F. Parisen Toldin, A. Pelissetto, and E. Vicari, J. Stat. Mech.: Theory Exp. (2007) P02016.
[15] N. G. Fytas and P. E. Theodorakis, Phys. Rev. E **82**, 062101 (2010).
[16] J. S. Wang, W. Selke, V. I. S. Dotsenko, and V. B. Andreichenko, Phys. A (Amsterdam, Neth.) **164**, 221 (1990).
[17] H.-O. Heuer, Phys. Rev. B **45**, 5691 (1992).
[18] O. G. Mouritsen and P. J. Shah, Phys. Rev. B **40**, 11445(R) (1989).
[19] Y. Tomita and Y. Okabe, Phys. Rev. E **64**, 036114 (2001).
[20] H. K. Janssen, K. Oerding, and E. Sengespeick, J. Phys. A: Math. Gen. **28**, 6073 (1995).
[21] H. O. Heuer, J. Phys. A: Math. Gen. **26**, L333 (1993).
[22] E. Domany, J. Phys. C: Solid State Phys. **12**, L119 (1979).
[23] C. K. Harris and R. B. Stinchcombe, Phys. Rev. Lett. **50**, 1399 (1983).
[24] S Jain, J. Phys. A: Math. Gen. **19**, L667 (1986).
[25] V. V. Prudnikov and O. N. Markov, Europhys. Lett. **29**, 245 (1995).
[26] G. Parisi, F. Ricci-Tersenghi, and J. J. Ruiz-Lorenzo, Phys. Rev. E **60**, 5198 (1999).
[27] D. Ivaneyko, J. Ilnytskyi, B. Berche, and Y. Holovatch, Phys. A (Amsterdam, Neth.) **370**, 163 (2006).
[28] M. Henkel and M. Pleimling, Phys. Rev. B **78**, 224419 (2008).
[29] E. Lippiello, A. Mukherhjee, S. Puri, and M. Zannetti, Europhys. Lett. **90**, 46006 (2010).
[30] M. P. Nightingale and H. W. J. Blöte, Phys. Rev. Lett. **76**, 4548 (1996).
[31] W. Zhong, D. Panja, G. T. Barkema, and R. C. Ball, Phys. Rev. E **98**, 012124 (2018).
[32] I. A. Hadjiagapiou, Phys. A (Amsterdam, Neth.) **390**, 1279 (2011).
[33] J. J. Binney, N. J. Dowrick, A. J. Fisher, and M. E. Newman, *The Theory of Critical Phenomena* (Clarendon Press, Oxford, 1995).
[34] H. Nishimori, J. Phys. C: Solid State Phys. **12**, L641 (1979).
[35] K. Binder, Z. Phys. B: Condens. Matter Quanta **43**, 119 (1981).
[36] U. Wolff, Phys. Rev. Lett. **62**, 361 (1989).
[37] M. E. J. Newman and G. T. Barkema, *Monte Carlo Methods in Statistical Physics* (Oxford University Press, Oxford, 1999).
[38] M. Ohzeki, Phys. Rev. E **79**, 021129 (2009).
[39] A. B. Harris, J. Phys. C: Solid State Phys. **7**, 1671 (1974).
[40] F. D. A. Aarão Reis, S. L. A. de Queiroz, and R. R. dos Santos, Phys. Rev. B **56**, 6013 (1997).